



1 **Differentiating local and regional sources of Chinese urban air pollution based on**  
2 **effect of Spring Festival**

3

4 Chuan Wang, Xiao-Feng Huang\*, Qiao Zhu, Li-Ming Cao, Bin Zhang, Ling-Yan He

5

6 Key Laboratory for Urban Habitat Environmental Science and Technology, School of Environment and Energy,  
7 Peking University Shenzhen Graduate School, Shenzhen, 518055, China.

8

9 \*Corresponding author: [huangxf@pku.edu.cn](mailto:huangxf@pku.edu.cn)

10

11 **Abstract:** The emission of pollutants is extremely reduced during the annual Chinese Spring Festival  
12 (SF) in Shenzhen, China. During the SF, traffic flow drops by ~50% and the industrial plants are almost  
13 entirely shut down in Shenzhen. To characterize the variation in ambient air pollutants due to the  
14 “Spring Festival effect”, various gaseous and particulate pollutants were measured in real time in urban  
15 Shenzhen over three consecutive winters (2014–2016). The results indicate that the concentrations of  
16 NO<sub>x</sub>, volatile organic compounds (VOCs), black carbon (BC), primary organic aerosols, chloride, and  
17 nitrate in submicron aerosols decrease by 50%–80% during the SF period relative to the non-Spring  
18 Festival periods, regardless of meteorological conditions, which suggests that these pollutants are  
19 mostly emitted or secondarily formed from urban local emissions. The concentration decreasing of  
20 regional pollutants or species emitted from natural sources, however, is found to be much less,  
21 especially for bulk PM<sub>2.5</sub> (–24%) and O<sub>3</sub> (6%). More detailed analysis of the Spring Festival effect  
22 reveals an urgent need to reduce emissions of SO<sub>2</sub> and VOCs on a regional scale rather than on an  
23 urban scale to reduce urban PM<sub>2.5</sub> in Shenzhen, which can also produce some use for reference for  
24 other megacities in China.



25 **Key words:** Spring Festival effect; local emissions; regional pollution; PM<sub>2.5</sub>; ozone

## 26 **1 Introduction**

27 The rapid economic development and urbanization of China over the recent decades has brought with  
28 it the consequence of severe atmospheric pollution, especially in the key economically developed  
29 regions, such as the Beijing–Tianjin–Hebei region (Sun et al., 2013, 2015; Guo et al., 2014), the  
30 Yangtze River Delta (Huang et al., 2013), and the Pearl River Delta (PRD), as well as their densely  
31 populated megacities (Hagler et al., 2006; Zhang et al., 2008; He et al., 2011). Great efforts have been  
32 made to determine the sources and formation mechanisms of fine particles (PM<sub>2.5</sub>) in these region.  
33 Previous studies indicate that PM<sub>2.5</sub> forms from primary fine particles and through secondary formation  
34 from gaseous precursors (Zhang et al., 2008; Zheng et al., 2009; Huang et al., 2014), and the sources  
35 of local production and regional transport are both important (Huang et al., 2014; Huang et al., 2006,  
36 2011; Li et al., 2015).

37

38 The causes of air pollution in urban atmosphere in China are particularly complicated, and bring great  
39 challenges to management strategies for protecting human health (Parrish and Zhu, 2009). To explore  
40 the causes of urban air pollution in China, previous studies have focused on monitoring and comparing  
41 the reduction in emissions during special events, such as the 2008 Beijing Olympic Games (Huang et  
42 al., 2010), the 2010 Guangzhou Asian Games (Xu et al., 2013), the 2014 Asia Pacific Economic  
43 Cooperation conference (APEC) (Chen et al., 2015; Sun et al., 2016; Zhang et al., 2016) and the 2015  
44 China victory day parade (Zhao et al., 2016). During such events, the air quality improved remarkable  
45 because of short-term limitations on traffic and industrial activity (Huang et al., 2010; Wang et al.,  
46 2010; Xu et al., 2013; Sun et al., 2016; Zhao et al., 2016). However, these limitations were temporary,



47 non-repeatable measures, so the reported emission reductions cannot be verified. Actually, a  
48 spontaneous reduction in emissions occurs every year in China during the Spring Festival (SF), which  
49 is the single most important holiday in China. During the week-long holiday (in January or February  
50 every year), the urban emission patterns depart significantly from the usual patterns: traffic decreases  
51 in the mega cities because most people are not working, and most of the industries, stores, and  
52 production sites are closed in the city except for the utilities and industries (e.g., power plants) that  
53 cannot be shut down (Qin et al., 2004; Feng et al., 2012; Shi et al., 2014). Tan et al. (2009) reported  
54 that the concentrations of NO<sub>x</sub>, CO, NMHC, SO<sub>2</sub>, and PM<sub>10</sub> were lower in the SF periods than in the  
55 non-Spring Festival (NSF) periods in the metropolitan area of Taipei over 1994-2006, while the  
56 variation of O<sub>3</sub> was in a reversed trend. Jiang et al. (2015) found that the ambient concentrations of  
57 VOCs had a sharp decline by ~60% during the SF in Shijiazhuang.

58

59 This study focuses on Shenzhen as a special example to evaluate the effect on urban air pollution of  
60 the SF. Shenzhen is in the eastern Pearl River Delta (PRD) and is the fourth largest economic center  
61 in China, with a total residential population of over 10 million and a fleet of civilian vehicles of more  
62 than 3.1 million (Shenzhen Yearbook of Statistics, 2015). Known as the country's city of most floating  
63 population, Shenzhen owns 7.4 million immigrants in 2014, which accounts 70% of the city's total  
64 population (Shenzhen Yearbook of Statistics, 2015). During the SF period, over 50% of the residents  
65 in Shenzhen are used to travel back to their hometowns (<http://sz.gov.cn>). It is reported that the traffic  
66 flow in Shenzhen during the SF of 2016 (Feb 7–13) was only the half before the SF period  
67 (<http://sz.gov.cn>). Additionally, industrial activities are almost totally suspended in Shenzhen during  
68 the SF period. To characterize the air quality during such extreme reductions of anthropogenic



69 activities during the SF period in Shenzhen, various air pollutants in Shenzhen urban areas were  
70 comprehensively and systematically monitored in real time in winter for three consecutive years  
71 (2014–2016). The annual SF in Shenzhen thus provides an excellent spontaneous control experiment  
72 for local emissions, which could provide unique and valuable information regarding the sources of  
73 urban air pollution.

74

## 75 **2 Experimental methods**

### 76 **2.1 Monitoring sites and meteorological conditions**

77 The monitoring site (22°36'N, 113°54'E) was on the roof (20 m above ground level) of an academic  
78 building on the campus of Peking University Shenzhen Graduate School (PKUSZ) (Figure S1). No  
79 significant anthropogenic emission sources exist nearby. The sampling schedule ran roughly from late  
80 January to early March over 2014–2016, which includes the official SF holiday period and the prior  
81 and following periods. Our definition of the SF period follows that of the statutory public holiday  
82 calendar in China, and it is continuous seven days in each year. While the seven days immediately  
83 before or after the holidays are actually the transition periods between the holidays and normal days  
84 (called the Tran. periods hereafter), when people begin to move from the city (or their hometowns) to  
85 their hometowns (or the city), the typical non-spring festival (NSF) periods are better defined as the  
86 7–14 days close to the SF period (called the NSFT period hereafter, where T indicates time similar).  
87 The specific dates and the average meteorological parameters are listed in Table 1, and Figure S2  
88 shows wind rose plots. The data in Table 1 show that the meteorology differs among the SF, NSFT,  
89 and Tran. periods. To control for the influence of meteorology on the evaluation of emissions, we  
90 selected another 7-day period each year when the meteorology is similar to that of the SF period (called



91 the NSFm period hereafter, where M indicates meteorology similar); the detailed parameters are listed  
 92 in Table 1 and Figure S2. The meteorological data for the SF period are fairly similar to those of the  
 93 NSFm period, suggesting similar meteorological conditions.

94

95 **Table 1.** Summary of meteorological conditions at sampling site during the SF, NSFT, NSFm and  
 96 Tran. periods of 2014–2016.

|                              |                                    | SF            | Tran.         | NSFT          | NSFM          |
|------------------------------|------------------------------------|---------------|---------------|---------------|---------------|
| Data period                  | 2014                               | Jan 31–Feb 6  | Feb 7–Feb 13  | Feb 14–Feb 20 | Feb 20–Feb 26 |
|                              | 2015                               | Feb 18–Feb 24 | Feb 11–Feb 17 | Feb 4–Feb 10  | Jan 24–Jan 30 |
|                              | 2016                               | Feb 7–Feb 13  | Feb 14–Feb 20 | Feb 21–Feb 27 | Feb 27–Mar 4  |
|                              | Temperature (°C)                   | 19.0±4.7      | 14.1±5.3      | 14.1±4.0      | 18.1±3.8      |
|                              | RH (%)                             | 68.1 ±17.8    | 69.3±18.4     | 64.9±16.7     | 67.4±14.7     |
|                              | Wind speed<br>(m s <sup>-1</sup> ) | 0.88 ±0.57    | 0.81±0.49     | 0.83±0.48     | 0.86±0.55     |
| Meteorological<br>parameters | Dominant wind<br>direction         | NW            | NW and NE     | NW and NE     | NW            |
|                              | Precipitation<br>(mm)              | 0             | 0             | 0             | 0             |
|                              | UVA (W m <sup>-2</sup> )           | 5.4±8.5       | 2.5±4.3       | 3.8±6.7       | 5.0±8.0       |
|                              | UVB (W m <sup>-2</sup> )           | 0.24±0.40     | 0.11±0.25     | 0.16±0.32     | 0.22±0.38     |



## 97 2.2 Instrumentation

98 For the ambient sampling in this study, the measuring instruments were placed in a room on the top  
99 floor of a four-story teaching building at PKUSZ. A high-sensitivity proton transfer reaction mass  
100 spectrometer (PTR-MS) (Ionicon Analytik GmbH, Austria) was used to measure the selected volatile  
101 organic compounds (VOCs). The PTR-MS measured a total of 25 masses in the selected ion mode at  
102 a time resolution of 30 s. Background checks were done for 30 of every 300 scan cycles with an  
103 activated charcoal trap at 360 °C, which can remove VOCs from the ambient air without changing  
104 water content. The VOCs reported here (Table S1) may be broadly classified into three categories:  
105 oxygenated VOCs [OVOCs: methanol, acetone, methyl ethyl ketone (MEK), acetaldehyde, and acetic  
106 acid], aromatics (benzene, toluene, styrene, C8 and C9 aromatics), and three types of tracers [isoprene,  
107 acetonitrile, and dimethyl sulfide (DMS)]. The PTR-MS was calibrated every 5 to 7 days by using a  
108 TO15 mixture standard (Air Environmental Inc., US) and permeation tubes (Valco Instruments Co.  
109 Inc., US) (de Gouw and Warneke, 2007).

110

111 An aerodyne high-resolution time-of-flight aerosol mass spectrometer (HR-ToF-AMS) (Aerodyne  
112 Research, US) was deployed to measure non-refractory PM<sub>1</sub> (NR-PM<sub>1</sub>) (Canagaratna et al., 2007) in  
113 the period 2014–2015 with a time resolution of 4 min. An aerosol chemical speciation monitor (ACSM)  
114 (Aerodyne Research, US) was used in 2016 with a dynamic resolution of 10 min. The detailed  
115 description of the ACSM is available in the recent review (Ng et al., 2011). The HR-ToF-AMS and  
116 ACSM were calibrated every month following the standard protocols (Ng et al., 2011; Jayne et al.,  
117 2000).

118



119 An aethalometer (AE-31) (Magee, US) was used for simultaneous detection of refractory black carbon  
120 (BC) with a time resolution of 5 min. In addition, a Scan Mobility Particle Sizer (TSI Inc., US) system  
121 was used to determine the particle number size distribution in the size range 15–615 nm (Stokes  
122 diameter) with a time resolution of 5 min. The stokes diameters of 15–615 nm is converted to  
123 aerodynamic diameters of 22–800 nm, and then  $PM_{0.8}$  mass concentration can be calculated with the  
124 particle density assumed according to the AMS measurement results of species.

125

126 To measure the  $PM_{2.5}$  mass concentration, we used a Thermo Scientific TEOM 1405-D monitor. The  
127 trace-gas instruments included a 43i sulfur dioxide ( $SO_2$ ) analyzer, a 42i nitric oxide (NO)–nitrogen  
128 dioxide ( $NO_2$ )–nitrogen oxide ( $NO_x$ ) analyzer, a 49i ozone ( $O_3$ ) analyzer, and a 48i carbon monoxide  
129 (CO) analyzer (Thermo Scientific, US). A meteorological station, also located on the roof of the same  
130 building, measured the main meteorological parameters, such as temperature, relative humidity, and  
131 wind speed (see Table 1).

132

### 133 **3 Results and Discussion**

#### 134 **3.1 The NSF–SF differences for major air pollutants**

135 The results of observations from 2014 to 2016 appear in Figures S3–S5. Figure 1 shows the averaged  
136 percent changes in the concentrations of major air pollutants of the SF periods relative to the two NSF  
137 periods and Tran. period over 2014–2016. The compounds  $m/z$  44 and  $m/z$  57 are the tracer of  
138 oxygenated organic aerosol and the tracer of primary hydrocarbon organic aerosol (Zhang et al., 2005),  
139 respectively, which are organic fragments in the AMS measurements. The notation  $O_3$ –8h refers to the  
140 average maximum  $O_3$  concentration over a continuous diurnal 8 h and  $PM_{0.8-2.5}$  refers to the difference



141 between the concentrations of  $PM_{2.5}$  and  $PM_{0.8}$ .

142

143 We can divide these air pollutants into three classes based on their percent changes: The group with  
144 the largest drop (hereinafter called “LD”) in concentration includes the aromatics (−50% to −88% for  
145 the various species, see Figure S6), OVOCs (−40% to −85% for the various species, see Figure S6),  
146  $NO_x$ , chloride (Chl), nitrate ( $NO_3^-$ ), BC, and  $m/z$  57. The concentrations of these pollutants all  
147 decrease by over 50% during the SF period compared with both the NSF periods. Apparently, the  
148 dominant sources for most of these pollutants are primary local emissions, such as combustion sources  
149 for BC,  $m/z$  57, and  $NO_x$  (Zhang et al., 2005; Kuhlbusch et al., 1998; Lan et al., 2011), and vehicle,  
150 industrial and solvent use for aromatics (Liu et al., 2008). As detailed in the following section, the  
151 diurnal patterns and relationships with respect to wind speed further confirm the sources of these  
152 pollutants. The dramatic decrease in the ambient concentrations of these species is consistent with  
153 reduction in local anthropogenic activities in Shenzhen during the SF period. The SF causes a 50%  
154 decrease in urban traffic and temporarily closing of almost all local industrial plants. The nitrate and  
155 chloride measured by AMS or ACSM are actually ammonium nitrate ( $NH_4NO_3$ ) and ammonium  
156 chloride ( $NH_4Cl$ ), which are typical secondary air pollutants. These are thought to form via reversible  
157 phase equilibria with gaseous ammonia ( $NH_3$ ), nitric acid ( $HNO_3$ ), and hydrochloric acid (HCl) (He et  
158 al., 2011; Huang et al., 2011; Zhang et al., 2007). Typically, the formation of  $NH_4NO_3$  from  $NO_x$  and  
159 the reaction between HCl and  $NH_3$  occur quickly in the atmosphere (Stelson and Seinfeld, 1982; Baek  
160 et al., 2004), suggesting that the concentrations of  $NO_3^-$  and Chl in winter in Shenzhen depend largely  
161 on the emission of precursors such as HCl and  $NO_x$ . Therefore, the significant decline in the ambient  
162 concentrations of  $NO_3^-$  and Chl during the SF period and indicates that their precursors also have local



163 origins, similar to the case for primary pollutants (this is also supported by the discussion in the  
164 following sections). The huge decline in the ambient concentration of OVOCs during the SF period  
165 shows that the source of these pollutants is (i) mainly from local emissions, including vehicle and  
166 industrial emissions (Schauer et al., 1999; Singh et al., 2001) and (ii) from secondary reactions  
167 involving local primary VOCs (Liu et al., 2015). Thus, in the LD group, the significant reduction in  
168 local sources of pollutants strongly impacts the concentration of air pollutants.

169

170 The pollutants in the next group undergo a medium drop in concentration during the SF period  
171 (hereinafter called “MD”). These are  $PM_{2.5}$ ,  $NR-PM_{10}$ ,  $PM_{0.8}$ , organic aerosol,  $m/z$  44, sulfate ( $SO_4^{2-}$ ),  
172 ammonium ( $NH_4^+$ ), isoprene, acetonitrile, DMS, and carbon monoxide (CO), and their percent change  
173 varies from  $-20\%$  to  $-55\%$  when comparing the SF periods to the NSFT and NSFPM periods. The  
174 species in this group are either typical secondary regional air pollutants, such as CO, which has a long  
175 lifetime and is a tracer for combustion sources, acetonitrile from rural biomass burning (de Gouw et  
176 al., 2003; Le Breton et al., 2013),  $m/z$  44 representing secondary organic aerosols,  $SO_4^{2-}$  from  $SO_2$   
177 oxidation (He et al., 2011; Huang et al., 2011), or typical tracers for natural sources, such as isoprene  
178 from vegetation (Guenther et al., 1995) and DMS from marine source (Dacey and Wakeham, 1986).  
179 In winter, the northeastern monsoon prevails in the PRD and transports significant amounts of various  
180 air pollutants from the northern inland, increasing air pollution of the PRD to the highest levels through  
181 the year (Huang et al., 2014). In particular, the small drop in CO concentration during the SF period  
182 puts it in this group and indicates that the contribution to regional air pollution does not decrease  
183 significantly during the SF period. Note that, the significant declines of the concentrations of isoprene  
184 and DMS imply that they have anthropogenic sources, which will be supported in the following



185 sections. The other air pollutants in this group are the reflection of the overall effect of the reduction  
186 of relevant air pollutants: OA is the whole of the two types of organic aerosol represented by m/z 44  
187 and m/z 57,  $\text{NH}_4^+$  is represented by  $\text{SO}_4^{2-}$ ,  $\text{NO}_3^-$  and Chl, and  $\text{NR-PM}_1$  is the sum of all species  
188 measured by AMS or ACSM (their average chemical compositions during different periods are shown  
189 in Figure S3–S5).

190

191 The group of pollutants with smallest decrease in concentration (hereinafter called “SD”) includes  $\text{SO}_2$ ,  
192  $\text{PM}_{0.8-2.5}$ , and  $\text{O}_3$ . The magnitude of the average percent change is less than 20% relative to the two  
193 NSF periods. The average concentration of  $\text{SO}_2$  was only 2.8 ppbv in Shenzhen in 2015  
194 (<http://www.szhec.gov.cn/>), which is much lower than that in Beijing (4.7 ppbv) and elsewhere in  
195 China (<http://www.zhb.gov.cn/>). This result is partly attributed to the negligible coal consumption in  
196 Shenzhen, which instead relies mainly on natural gas and liquefied petroleum gas (Shenzhen Yearbook  
197 of Statistics, 2015). The emission inventory indicates that international marine container vessels are  
198 the dominant source of  $\text{SO}_2$  in Shenzhen (Wang et al., 2009), and according to official statistics, the  
199 Shenzhen port piloted 401, 568, and 521 ships during the SF period in the years 2014–2016,  
200 respectively, which is quite similar to numbers for the NSF periods (<http://www.pilot.com.cn/>).  
201 Obviously, the small decrease of  $\text{SO}_2$  is reasonably related with the stable ship emissions during the  
202 SF periods. The small decline of  $\text{PM}_{0.8-2.5}$  during the SF period suggests that the reduction of more  
203 aged particles of larger sizes in  $\text{PM}_{2.5}$  is much lower than fresher particles of smaller size. This can be  
204 also confirmed by particle number concentration (PNC) measurement by SMPS, as shown in Figure  
205 2. The largest difference of the PNC between the SF and NSF periods exists mainly in a smaller size  
206 range (20–40 nm), which is recognized as the nucleation mode or second Aitken mode that represents



207 fresh combustion emission (Ferin et al., 1990). Contrary to other pollutants, the concentrations of O<sub>3</sub>,  
208 present small increasing during the SF period (except a little decline when comparing O<sub>3</sub>-8h with the  
209 NSFm period), which could be attributed to the different drop rates for O<sub>3</sub> precursor species, i.e. NO<sub>x</sub>  
210 and VOCs (Qin et al., 2004), and will be discussed in more detail in section 3.2.

211

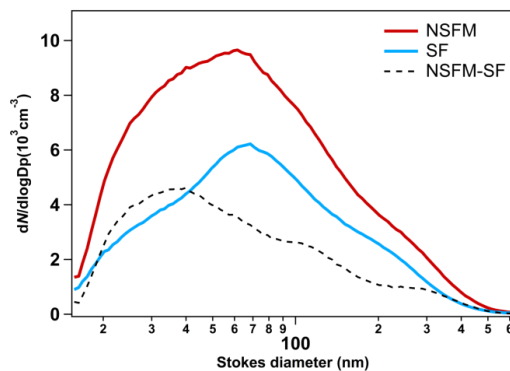
212 The results for the various species during the NSFT and NSFm periods are consistent, which suggest  
213 that meteorology has only a small impact on their concentrations. This means that the strong decrease  
214 in the concentrations of air pollutants in group LD and MD is mainly due to the abatement of local  
215 sources. The larger decline in the SF period when compared to NSFT than to NSFm is associated with  
216 the lower temperature and stronger winds from the polluted northwest inland of the PRD during the  
217 NSFT period. In addition, the effect of the SF on the concentrations of the various species is almost  
218 identical each year (see Figure S7), which further confirms that the pollutant concentrations are  
219 determined primarily by the activity of the sources. In Figure 1, the percent changes of pollutants of  
220 the SF periods relative to the Tran. periods are also presented, and it is found that the three-group  
221 classification defined above is also applicable, while the decrease levels are lower. For example, the  
222 average decrease percent of Group LD for the Tran. period case is 61%, while those for the NSFT and  
223 NSFm cases are 71% and 63%, respectively. This result is consistent with the fact that the SF travel  
224 of people occurred mostly during the seven days before and after the SF holidays (<http://sz.gov.cn>),  
225 and thus the city became much emptier even in the Tran. periods. In order to make a deeper and valid  
226 comparison for revealing the SF effect, the following discussion will only take the NSFm periods and  
227 SF periods for comparative analysis due to their more similar meteorology.



228

229 **Figure 1.** Percent change in concentrations of major air pollutants during the SF period relative to (a)

230 Tran., (b) NSFT and (c) NSFM periods averaged over 2014–2016.



231

232 **Figure 2.** Distribution of particle number concentration in the 15–615 nm size range during the SF

233 and NSFM periods.

234



### 235 **3.2 The diurnal variation of major air pollutants**

236 As shown in Figure 3, the diurnal cycles of all LD pollutants (except for the OVOCs) reveal significant  
237 peaks in concentration around 8–9 am in the NSFM period, which is attributed to the low planetary  
238 boundary layer (PBL) in the morning and local rush hour traffic emissions. The evening rush hour  
239 peak, however, is not apparent for all the species, which is attributed to the higher ambient temperature  
240 and thus the higher PBL at that time than in the morning. During the SF period, the concentrations of  
241 all pollutants are far lower over the entire day. In particular, the rush-hour peaks become much smaller  
242 or disappear altogether, which is consistent with the large reduction in local vehicle emissions during  
243 the SF period. Although the sources of Chl remained uncertain in previous studies (Huang et al., 2011;  
244 Aiken et al., 2008), the maximal reduction (80%) in this pollutant during the morning rush hour during  
245 the SF period implies that local traffic emissions account for a significantly fraction of this pollutant  
246 in Shenzhen (Figure 3E). Contrary to other species in this group, the concentration of OVOCs is high  
247 in the daytime and peaks in the morning after the morning rush hour time during the NSFM period  
248 (Figure 3D), suggesting that photochemical production and/or daytime industrial activities may be  
249 important sources of OVOCs. The concentrations of different aromatics and OVOCs usually follow  
250 similar diurnal variations (Figure S8).

251

252 The diurnal variations of the MD pollutants are relatively smooth except for the two natural VOCs  
253 (isoprene and DMS; see Figures 3L and 3M), which indicates that these pollutants come from regional  
254 sources and are dispersed more uniformly over a larger scale. The apparent difference of the diurnal  
255 variations of those anthropogenic air pollutants between the SF and NSFM periods also exists in the  
256 rush hours (except for acetonitrile; Figure 3J), however, the reduction in local sources has a relatively



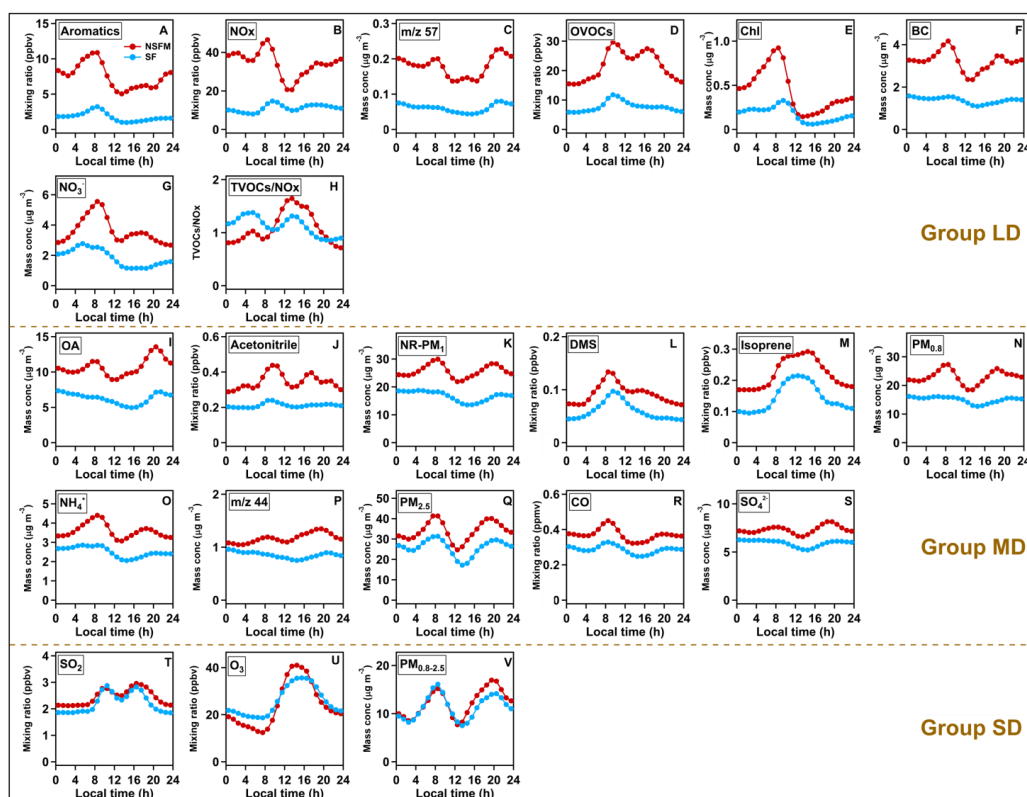
257 weak effect on the overall concentrations of these pollutants. Acetonitrile, which is a tracer of biomass  
258 burning, is more concentrated during the daytime and its peak concentration occurs after the rush hours  
259 during the NSF period (Figure 3J), which is similar to the result obtained for OVOCs and may be  
260 attributed to the influence of daytime anthropogenic activities, for example, industrial biomass boilers.  
261 Isoprene is primarily emitted by vegetation as a function of light and temperature, so the concentration  
262 of this pollutant goes through a broad peak that spans the daytime hours during both the NSF and  
263 SF periods. The percent change in isoprene concentration between the SF and NSF periods is  
264 approximately -40% (Figure 3M), despite the NSF and SF periods having similar temperature and  
265 solar radiation, which implies that the contribution of anthropogenic sources to isoprene cannot be  
266 overlooked in Shenzhen. Many studies have reported isoprene from vehicle exhaust, especially in cold  
267 seasons (Barletta et al., 2005; Borbon et al., 2001). DMS is reported to be a marine tracer (Dacey et  
268 al., 1986), its peak concentration occurs in the morning during both the NSF and SF periods (Figure  
269 3L), which is presumably related to the minimal PBL. The concentration of DMS decreases by 30%–  
270 50% during the SF period, which reflects the reduced DMS emissions from anthropogenic sources. As  
271 reported in the literature, industrial activities can make significant emissions of DMS (Schafer et al.,  
272 2010).

273

274 The diurnal variations of  $PM_{0.8-2.5}$ ,  $SO_2$  and  $O_3$  demonstrated more similar concentrations and trends  
275 in the SF and NSF periods, respectively (Figure 3T–3V). For  $PM_{0.8-2.5}$ , a small difference is found  
276 in the afternoon, which is supposed to be a result of more aged larger particles formed through stronger  
277 photochemical reactions during the NSF period. Though, slight differences appear in  $SO_2$   
278 concentration, mainly during the nighttime when the PBL is low. These data suggest a minor role of



279 local near-ground SO<sub>2</sub> sources, such as vehicles. Although the daytime peak concentration of O<sub>3</sub> during  
280 the NSF<sub>M</sub> period is slightly greater than that during the SF period, this trend reverses from the evening  
281 to the midmorning hours. Similar phenomena have also been observed in other emission-reduction  
282 studies of urban areas (i.e., emissions are greater on holidays than on non-holidays) (Qin et al., 2004;  
283 Tan et al., 2009). In addition, emissions were higher during the 2008 Beijing Olympic Games (Chou  
284 et al., 2011), during which strict controls were imposed. A recent study reported that, in most of the  
285 PRD region, O<sub>3</sub> formation is VOC limited in the morning and becomes NO<sub>x</sub> limited during peak O<sub>3</sub>  
286 hours (Li et al., 2013). The concentrations of NO<sub>x</sub> and VOCs decrease gradually from 8 to 12 h during  
287 the SF period whereas the concentration ratio TVOC/NO<sub>x</sub> increases (see Figure 3H, where TVOC  
288 concentration is the sum of aromatic and OVOC concentrations). Thus, the lack of NO<sub>x</sub> at noon during  
289 the SF period hinders the generation of O<sub>3</sub>. At other hours in the NSF<sub>M</sub> period, a higher NO  
290 concentration destroys O<sub>3</sub>, implying that the oxidation reaction with NO may produce a titration effect  
291 (Qin et al., 2004; Tan et al., 2009). As a result, although the reduction in emissions of urban  
292 anthropogenic sources leads to a significant decline of NO<sub>x</sub> and VOCs, this reduction does not mitigate  
293 the average ambient O<sub>3</sub> concentration, which implies that the concentration ratio VOC/NO<sub>x</sub> plays an  
294 important role in controlling O<sub>3</sub> concentration.



295

296 **Figure 3.** Diurnal variations in concentrations of major air pollutants at PKUSZ site over the SF  
297 (blue dots) and NSFM (red dots) periods.

298

### 299 3.3 Influence of wind on observed air pollutants

300 Wind plays a crucial role in the dilution and transport of air pollution. The wind field is essentially the  
301 same during the SF and NSFM periods. In general, the concentrations of LD air pollutants depend  
302 strongly on wind speed during the NSFM period, whereas this dependence becomes much weaker  
303 during the SF period (Figure 4). The difference in the concentration of LD air pollutants (including  
304 various aromatics and OVOCs, see Figure S9) between the NSFM and SF periods is maximal (50%–  
305 80%) under conditions of low wind speeds (<1 m/s) because local pollution can more easily



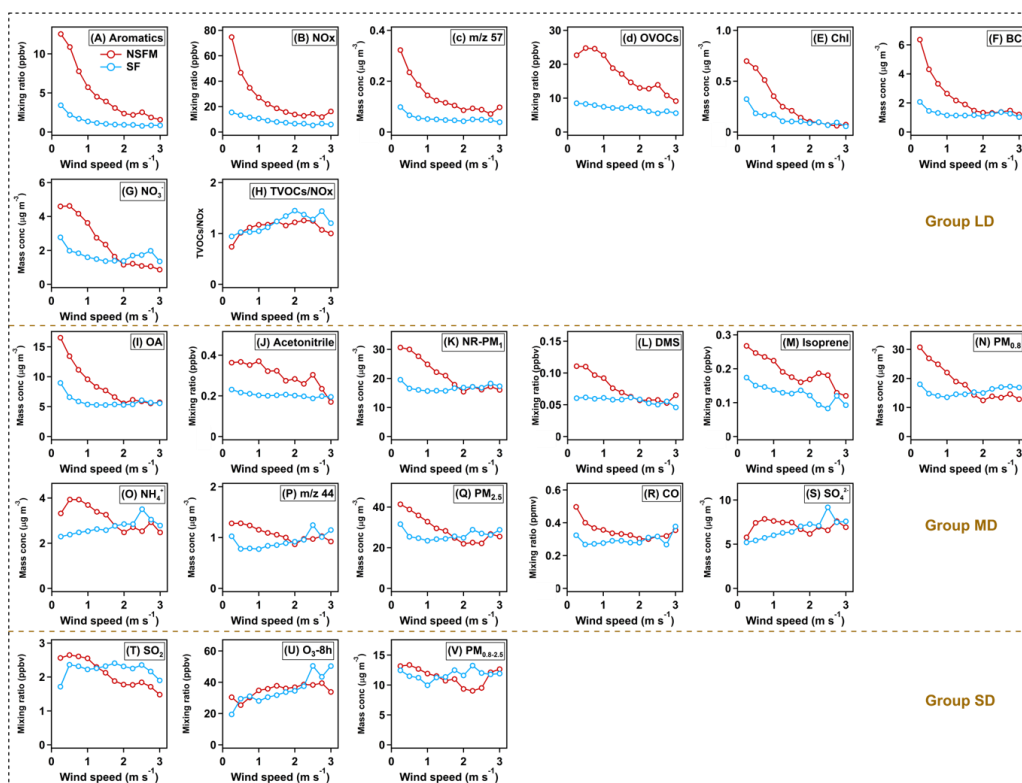
306 accumulate under these conditions. These results confirm that the concentration of air pollutants from  
307 local sources is strongly reduced during in the SF period.

308

309 Compared with the LD pollutants, the concentrations of CO,  $\text{SO}_4^{2-}$ , m/z 44, isoprene, DMS, and  
310 acetonitrile do not vary significantly with wind speed during the NSFPM period, providing further  
311 evidence that these pollutants come from regional or natural sources and are consequently more evenly  
312 distributed in the atmosphere.

313

314 In the Group SD,  $\text{SO}_2$  is generally little influenced by wind speed during the SF period, while some  
315 higher concentrations appeared under low wind speeds during the NSFPM period, indicating again small  
316 contribution of urban local sources to  $\text{SO}_2$ . The fluctuation of  $\text{PM}_{0.8-2.5}$  both in the SF and NSFPM  
317 periods does not reveal a clear relationship with wind speed, suggesting again it is not a typical locally  
318 emitted air pollutant. The variations of  $\text{O}_3-8\text{h}$  display the opposite trend to other air pollutants both in  
319 the SF and NSFPM periods, growing smoothly as wind speed increases, which could be possibly  
320 attributed to more regional transport and/or the higher VOCs/ $\text{NO}_x$  ratio under high wind speeds  
321 (Figure 4H). Note that, when the proportion of regional transport relative to local emission becomes  
322 bigger under higher wind speeds, the concentrations of  $\text{NO}_3^-$ ,  $\text{SO}_4^{2-}$ , m/z 44,  $\text{PM}_{0.8-2.5}$ , and  $\text{O}_3-8\text{h}$  are  
323 even slightly higher in the SF period than in the NSFPM period, implying that regional photochemical  
324 production during the SF period is not weakened.



325

326 **Figure 4.** Concentrations of major air pollutants as a function of wind speed during the SF and  
 327 NSFm periods.

328

### 329 3.4 Emission ratio analysis

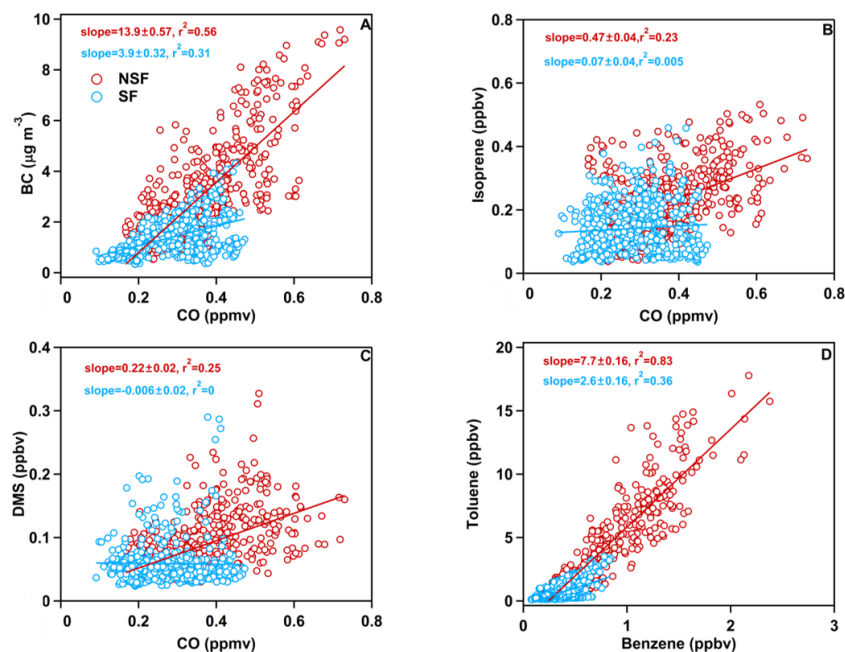
330 Several groups of special correlations were applied to analyze the source characteristics of air  
 331 pollutants in Figure 5. CO and BC are both products of incomplete combustion (Subramanian et al.,  
 332 2010), but gaseous CO can travel farther because of its longer atmospheric lifetime (approximately a  
 333 month for CO vs a week for BC) (Khalil et al., 1990; Ogren et al., 1983). As shown in Figure 5A, the  
 334 correlation coefficient and slope between BC and CO during the NSFm period ( $r^2 = 0.56$ , slope = 13.9)



335 is greater than during the SF period ( $r^2 = 0.31$ , slope = 3.9), suggesting that local combustion sources  
336 make a much greater contribution during the NSF period, but decline significantly during the SF  
337 period (He et al., 2011). The concentrations of two natural species, isoprene and DMS, are not  
338 correlated with CO during the SF, whereas their correlation with CO is non-negligible during the  
339 NSF period (Figures 5B and 5C), suggesting again that these pollutants have an anthropogenic  
340 source during the NSF period.

341

342 The toluene/benzene ratio can be used to estimate the contribution of traffic emissions (Schneider et  
343 al., 2005). Generally, a value of 1.2–3 is found to be characteristic of vehicular emission in many urban  
344 areas (Nelson et al., 1984; Wang et al., 2002; Araizaga et al., 2013). The lower ratio of toluene to  
345 benzene (ave.=2.6) in the SF period suggests that the dominant source is vehicle emission. This ratio  
346 in the NSF period, however, is much higher (ave.=7.7), indicating more complicated sources of  
347 VOCs like huge amount of toluene solvent usage in industrial activities in PRD (Barletta et al., 2005,  
348 2008; Chan et al., 2006). This finding is well consistent with the temporary closure of industrial plants  
349 in the SF period, which leads to little toluene emission.



350

351 **Figure 5.** Correlation between air pollutants (A) BC and CO (B) isoprene and CO, (C) DMS and  
352 CO, and (D) toluene and benzene during the SF (blue circles) and the NSF (red circles) periods.

353

### 354 3.5 Conclusions

355 This study uses the SF in Shenzhen to investigate how the urban air quality reacts to significant,  
356 temporary reductions in emission. During the winters of 2014 to 2016, the air quality was observed  
357 continuously at Peking University Shenzhen Graduate School, from which we obtained the percent  
358 change in the concentrations of various air pollutants during the SF periods with respect to the  
359 comparable NSF periods. The analysis of these data shows that, despite meteorological variations, the  
360 Spring Festival clearly and consistently influences the urban concentrations of various air pollutants.

361 The air pollutants can be divided into three groups: the large-decrease (LD) pollutants are those with



362 a percent change in concentration of  $-50\%$  to  $-80\%$  during the SF period and include aromatics,  $\text{NO}_x$ ,  
363  $m/z$  57, OVOCs, Chl, BC, and  $\text{NO}_3^-$ . These results are consistent with the variation in urban emission  
364 sources during the SF, suggesting that these pollutants are mostly directly emitted or formed from  
365 secondary reactions between locally emitted pollutants. The medium-decrease (MD) pollutants are  
366  $\text{PM}_{2.5}$ ,  $\text{NR-PM}_1$ ,  $\text{PM}_{0.8}$ , organic aerosol,  $m/z$  44,  $\text{SO}_4^{2-}$ ,  $\text{NH}_4^+$ , isoprene, acetonitrile, DMS, and CO;  
367 the concentrations of these pollutants decrease by 20% to 55% during the SF, which indicates that the  
368 extreme reduction in urban emissions during the SF period has limited effect on regional or natural air  
369 pollutants. These results provide further evidence that the origins of these pollutants are primarily  
370 regional or natural. Finally, the slight-decrease (SD) pollutants include  $\text{SO}_2$ ,  $\text{PM}_{0.8-2.5}$ , and  $\text{O}_3$ . The  
371 average percent change in the concentrations of these pollutants during the SF period is less than 20%,  
372 which indicates that a significant reduction in urban emissions does not significantly affect their  
373 concentration. Of particular interest is the origin of  $\text{PM}_{0.8-2.5}$ , which is almost completely regional. In  
374 addition, it is found that the concentration of  $\text{O}_3$ -8h correlates strongly with the concentration ratio  
375  $\text{TVOC}/\text{NO}_x$ .

376

377 The results of this study show that the extreme reductions in urban emissions of Shenzhen only affects  
378 the concentration of smaller fresh particles, such as  $\text{PM}_{0.8}$ , whereas the reduction of  $\text{PM}_{2.5}$  is only  
379 slightly affected because of the weak influence on aged, larger particles such as  $\text{PM}_{0.8-2.5}$ . The  
380 concentrations of  $\text{SO}_4^{2-}$  and secondary organic aerosols are hardly unaffected by local reductions in  
381 emissions. Therefore, reducing the emissions of  $\text{SO}_2$  and VOCs on a regional scale is critical for  
382 reducing their concentrations and achieving the goal of reducing concentrations of  $\text{PM}_{2.5}$ , at least for  
383 South China. On the other hand,  $\text{O}_3$  has recently become an increasingly important air pollutant in



384 China, especially in the PRD. However, the significant reduction of the concentration of its precursors  
385 (NO<sub>x</sub> and VOCs) during the SF period does not lead to significant reduction of the O<sub>3</sub> concentration  
386 because of the concentration ratio VOCs/NO<sub>x</sub> remains unchanged. Consequently, further  
387 investigations are required to control not only the emissions of VOCs and NO<sub>x</sub> but also their  
388 concentration ratio.

389

### 390 **Acknowledgements**

391 This work was supported by the National Natural Science Foundation of China (U1301234 &  
392 41622304), the Ministry of Science and Technology of China (2014BAC21B03), and the Science and  
393 Technology Plan of Shenzhen Municipality.

394

### 395 **Reference**

- 396 Aiken, A. C., Decarlo, P. F., Kroll, J. H., Worsnop, D. R., Huffman, J. A., Docherty, K. S., Ulbrich, I.  
397 M., Mohr, C., Kimmel, J. R., Sueper, D., Sun, Y., Zhang, Q., Trimborn, A., Northway, M., Ziemann,  
398 P. J., Canagaratna, M. R., Onasch, T. B., Alfarra, M. R., Prevot, A. S. H., Dommen, J., Duplissy, J.,  
399 Metzger, A., Baltensperger, U., and Jimenez, J. L.: O/C and OM/OC ratios of primary, secondary,  
400 and ambient organic aerosols with high-resolution time-of-flight aerosol mass spectrometry,  
401 *Environ. Sci. Technol.*, 42, 4478-4485, doi:10.1021/es703009q, 2008.
- 402 Araizaga, A. E., Mancilla, Y., and Mendoza, A.: Volatile Organic Compound Emissions from Light-  
403 Duty Vehicles in Monterrey, Mexico: a Tunnel Study, *Int. J. Environ. Res.*, 7, 277-292, 2013.
- 404 Baek, B. H., Aneja, V. P., and Tong, Q. S.: Chemical coupling between ammonia, acid gases, and fine  
405 particles, *Environ. Pollut.*, 129, 89-98, doi:10.1016/j.envpol.2003.09.022, 2004.
- 406 Barletta, B., Meinardi, S., Rowland, F. S., Chan, C. Y., Wang, X. M., Zou, S. C., Chan, L. Y., and Blake,  
407 D. R.: Volatile organic compounds in 43 Chinese cities, *Atmos. Environ.*, 39, 5979-5990,  
408 doi:10.1016/j.atmosenv.2005.06.029, 2005.



- 409 Barletta, B., Meinardi, S., Simpson, I. J., Zou, S. C., Rowland, F. S., and Blake, D. R.: Ambient mixing  
410 ratios of nonmethane hydrocarbons (NMHCs) in two major urban centers of the Pearl River Delta  
411 (PRD) region: Guangzhou and Dongguan, *Atmos. Environ.*, 42, 4393-4408,  
412 doi:10.1016/j.atmosenv.2008.01.028, 2008.
- 413 Borbon, A., Fontaine, H., Veillerot, M., Locoge, N., Galloo, J. C., and Guillermo, R.: An investigation  
414 into the traffic-related fraction of isoprene at an urban location, *Atmos. Environ.*, 35, 3749-3760,  
415 doi:10.1016/S1352-2310(01)00170-4, 2001.
- 416 Canagaratna, M. R., Jayne, J. T., Jimenez, J. L., Allan, J. D., Alfarra, M. R., Zhang, Q., Onasch, T. B.,  
417 Drewnick, F., Coe, H., Middlebrook, A., Delia, A., Williams, L. R., Trimborn, A. M., Northway, M.  
418 J., DeCarlo, P. F., Kolb, C. E., Davidovits, P., and Worsnop, D. R.: Chemical and microphysical  
419 characterization of ambient aerosols with the aerodyne aerosol mass spectrometer, *Mass Spectrom.*  
420 *Rev.*, 26, 185-222, doi:10.1002/mas.20115, 2007.
- 421 Chan, L. Y., Chu, K. W., Zou, S. C., Chan, C. Y., Wang, X. M., Barletta, B., Blake, D. R., Guo, H., and  
422 Tsai, W. Y.: Characteristics of nonmethane hydrocarbons (NMHCs) in industrial, industrial-urban,  
423 and industrial-suburban atmospheres of the Pearl River Delta (PRD) region of south China, *J.*  
424 *Geophys. Res.-Atmos.*, 111(D11), D11304, doi:10.1029/2005jd006481, 2006.
- 425 Chen, C., Sun, Y. L., Xu, W. Q., Du, W., Zhou, L. B., Han, T. T., Wang, Q. Q., Fu, P. Q., Wang, Z. F.,  
426 Gao, Z. Q., Zhang, Q., and Worsnop, D. R.: Characteristics and sources of submicron aerosols above  
427 the urban canopy (260m) in Beijing, China, during the 2014 APEC summit, *Atmos. Chem. Phys.*,  
428 15, 12879–12895, doi:10.5194/acp-15-12879-2015, 2015.
- 429 Chou, C. C. K., Tsai, C. Y., Chang, C. C., Lin, P. H., Liu, S. C., and Zhu, T.: Photochemical production  
430 of ozone in Beijing during the 2008 Olympic Games, *Atmos. Chem. Phys.*, 11, 9825-9837,  
431 doi:10.5194/acp-11-9825-2011, 2011.
- 432 Dacey, J. W. H., and Wakeham, S. G.: Oceanic Dimethylsulfide - Production during Zooplankton  
433 Grazing on Phytoplankton, *Science*, 233, 1314-1316, doi:10.1126/science.233.4770.1314, 1986.
- 434 de Gouw, J. A., Warneke, C., Parrish, D. D., Holloway, J. S., Trainer, M., and Fehsenfeld, F. C.:  
435 Emission sources and ocean uptake of acetonitrile (CH<sub>3</sub>CN) in the atmosphere, *J. Geophys. Res.-*  
436 *Atmos.*, 108, doi:10.1029/2002jd002897, 2003.
- 437 de Gouw, J., and Warneke, C.: Measurements of volatile organic compounds in the earths atmosphere  
438 using proton-transfer-reaction mass spectrometry, *Mass Spectrom. Rev.*, 26, 223-257,



- 439 doi:10.1002/mas.20119, 2007.
- 440 Feng, J. L., Sun, P., Hu, X. L., Zhao, W., Wu, M. H., and Fu, J. M.: The chemical composition and  
441 sources of PM<sub>2.5</sub> during the 2009 Chinese New Year's holiday in Shanghai, *Atmos. Res.*, 118, 435-  
442 444, doi:10.1016/j.atmosres.2012.08.012, 2012.
- 443 Ferin, J., Oberdorster, G., Penney, D. P., Soderholm, S. C., Gelein, R., and Piper, H. C.: Increased  
444 Pulmonary Toxicity of Ultrafine Particles .1. Particle Clearance, Translocation, Morphology, *J.*  
445 *Aerosol Sci.*, 21, 381-384, doi:10.1016/0021-8502(90)90064-5, 1990.
- 446 Guenther, A., Hewitt, C. N., Erickson, D., Fall, R., Geron, C., Graedel, T., Harley, P., Klinger, L.,  
447 Lerdau, M., Mckay, W. A., Pierce, T., Scholes, B., Steinbrecher, R., Tallamraju, R., Taylor, J., and  
448 Zimmerman, P.: A Global-Model Of Natural Volatile Organic-Compound Emissions, *J. Geophys.*  
449 *Res.-Atmos.*, 100, 8873-8892, doi:10.1029/94jd02950, 1995.
- 450 Guo, S., Hu, M., Zamora, M. L., Peng, J. F., Shang, D. J., Zheng, J., Du, Z. F., Wu, Z., Shao, M., Zeng,  
451 L. M., Molina, M. J., and Zhang, R. Y.: Elucidating severe urban haze formation in China, *P. Natl.*  
452 *Acad. Sci. USA*, 111, 17373-17378, doi:10.1073/pnas.1419604111, 2014.
- 453 Hagler, G. S., Bergin, M. H., Salmon, L. G., Yu, J. Z., Wan, E. C. H., Zheng, M., Zeng, L. M., Kiang,  
454 C. S., Zhang, Y. H., Lau, A. K. H., and Schauer, J. J.: Source areas and chemical composition of fine  
455 particulate matter in the Pearl River Delta region of China, *Atmos. Environ.*, 40, 3802-3815,  
456 doi:10.1016/j.atmosenv.2006.02.032, 2006.
- 457 He, L. Y., Huang, X. F., Xue, L., Hu, M., Lin, Y., Zheng, J., Zhang, R. Y., and Zhang, Y. H.: Submicron  
458 aerosol analysis and organic source apportionment in an urban atmosphere in Pearl River Delta of  
459 China using high-resolution aerosol mass spectrometry, *J. Geophys. Res.-Atmos.*, 116, D12304,  
460 doi:10.1029/2010jd014566, 2011.
- 461 Huang, R. J., Zhang, Y. L., Bozzetti, C., Ho, K. F., Cao, J. J., Han, Y. M., Daellenbach, K. R., Slowik,  
462 J. G., Platt, S. M., Canonaco, F., Zotter, P., Wolf, R., Pieber, S. M., Brun, E. A., Crippa, M., Ciarelli,  
463 G., Piazzalunga, A., Schwikowski, M., Abbaszade, G., Schnelle-Kreis, J., Zimmermann, R., An, Z.  
464 S., Szidat, S., Baltensperger, U., El Haddad, I., and Prevot, A. S. H.: High secondary aerosol  
465 contribution to particulate pollution during haze events in China, *Nature*, 514, 218-222,  
466 doi:10.1038/nature13774, 2014.
- 467 Huang, X. F., Yu, J. Z., He, L. Y., and Yuan, Z. B.: Water-soluble organic carbon and oxalate in aerosols  
468 at a coastal urban site in China: Size distribution characteristics, sources, and formation mechanisms,



- 469 J. Geophys. Res.-Atmos., 111, D22212, doi:10.1029/2006jd007408, 2006.
- 470 Huang, X. F., He, L. Y., Hu, M., Canagaratna, M. R., Sun, Y., Zhang, Q., Zhu, T., Xue, L., Zeng, L. W.,  
471 Liu, X. G., Zhang, Y. H., Jayne, J. T., Ng, N. L., and Worsnop, D. R.: Highly time-resolved chemical  
472 characterization of atmospheric submicron particles during 2008 Beijing Olympic Games using an  
473 Aerodyne High-Resolution Aerosol Mass Spectrometer, Atmos. Chem. Phys., 10, 8933-8945,  
474 doi:10.5194/acp-10-8933-2010, 2010.
- 475 Huang, X. F., He, L. Y., Hu, M., Canagaratna, M. R., Kroll, J. H., Ng, N. L., Zhang, Y. H., Lin, Y., Xue,  
476 L., Sun, T. L., Liu, X. G., Shao, M., Jayne, J. T., and Worsnop, D. R.: Characterization of submicron  
477 aerosols at a rural site in Pearl River Delta of China using an Aerodyne High-Resolution Aerosol  
478 Mass Spectrometer, Atmos. Chem. Phys., 11, 1865-1877, doi:10.5194/acp-11-1865-2011, 2011.
- 479 Huang, X. F., Xue, L., Tian, X. D., Shao, W. W., Sun, T. L., Gong, Z. H., Ju, W. W., Jiang, B., Hu, M.,  
480 and He, L. Y.: Highly time-resolved carbonaceous aerosol characterization in Yangtze River Delta  
481 of China: Composition, mixing state and secondary formation, Atmos. Environ., 64, 200-207,  
482 doi:10.1016/j.atmosenv.2012.09.059, 2013.
- 483 Huang, X. F., Yun, H., Gong, Z. H., Li, X., He, L., Zhang, Y. H., and Hu, M.: Source apportionment  
484 and secondary organic aerosol estimation of PM<sub>2.5</sub> in an urban atmosphere in China, Sci. China  
485 Earth Sci., 57, 1352-1362, doi:10.1007/s11430-013-4686-2, 2014.
- 486 Jayne, J. T., Leard, D. C., Zhang, X. F., Davidovits, P., Smith, K. A., Kolb, C. E., and Worsnop, D. R.:  
487 Development of an aerosol mass spectrometer for size and composition analysis of submicron  
488 particles, Aerosol Sci. Tech., 33, 49-70, doi:10.1080/027868200410840, 2000.
- 489 Jiang, J. B., Jin, W., Yang, L. L., Feng, Y., Chang, Q., Li, Y. Q., and Zhou, J. B.: The Pollution  
490 Characteristic of VOCs of Ambient Air in Winter in Shijiazhang, Environmental Monitoring in  
491 China, 31, 2015 (in Chinese).
- 492 Khalil, M. A. K., and Rasmussen, R. A.: The Global Cycle of Carbon-Monoxide-Trends And Mass  
493 Balance, Chemosphere, 20, 227-242, doi: 10.1016/0045-6535(90)90098-E, 1990.
- 494 Kuhlbusch, T. A. J.: Black carbon and the carbon cycle, Science, 280, 1903-1904,  
495 doi:10.1126/science.280.5371.1903, 1998.
- 496 Lan, Z. J., Chen, D. L., Li, X. A., Huang, X. F., He, L. Y., Deng, Y. G., Feng, N., and Hu, M.: Modal  
497 characteristics of carbonaceous aerosol size distribution in an urban atmosphere of South China,  
498 Atmos. Res., 100, 51-60, doi:10.1016/j.atmosres.2010.12.022, 2011.



- 499 Le Breton, M., Bacak, A., Muller, J. B. A., O'Shea, S. J., Xiao, P., Ashfold, M. N. R., Cooke, M. C.,  
500 Batt, R., Shallcross, D. E., Oram, D. E., Forster, G., Bauguitte, S. J. B., and Percival, C. J.: Airborne  
501 hydrogen cyanide measurements using a chemical ionisation mass spectrometer for the plume  
502 identification of biomass burning forest fires, *Atmos. Chem. Phys.*, 13, 9217-9232, doi:10.5194/acp-  
503 13-9217-2013, 2013.
- 504 Li, P. F., Yan, R. C., Yu, S. C., Wang, S., Liu, W. P., and Bao, H. M.: Reinstate regional transport of  
505 PM<sub>2.5</sub> as a major cause of severe haze in Beijing, *P. Natl. Acad. Sci. USA*, 112, E2739-E2740,  
506 doi:10.1073/pnas.1502596112, 2015.
- 507 Li, Y., Lau, A. K. H., Fung, J. C. H., Zheng, J. Y., and Liu, S. C.: Importance of NO<sub>x</sub> control for peak  
508 ozone reduction in the Pearl River Delta region, *J. Geophys. Res.-Atmos.*, 118, 9428-9443,  
509 doi:10.1002/jgrd.50659, 2013.
- 510 Liu, Y., Shao, M., Lu, S. H., Chang, C. C., Wang, J. L., and Fu, L. L.: Source apportionment of ambient  
511 volatile organic compounds in the Pearl River Delta, China: Part II, *Atmos. Environ.*, 42, 6261-6274,  
512 doi:10.1016/j.atmosenv.2008.02.027, 2008.
- 513 Liu, Y., Yuan, B., Li, X., Shao, M., Lu, S., Li, Y., Chang, C. C., Wang, Z., Hu, W., Huang, X., He, L.,  
514 Zeng, L., Hu, M., and Zhu, T.: Impact of pollution controls in Beijing on atmospheric oxygenated  
515 volatile organic compounds (OVOCs) during the 2008 Olympic Games: observation and modeling  
516 implications, *Atmos. Chem. Phys.*, 15, 3045-3062, doi:10.5194/acp-15-3045-2015, 2015.
- 517 Louie, P. K. K., Watson, J. G., Chow, J. C., Chen, A., Sin, D. W. M., and Lau, A. K. H.: Seasonal  
518 characteristics and regional transport of PM<sub>2.5</sub> in Hong Kong, *Atmos. Environ.*, 39, 1695-1710,  
519 doi:10.1016/j.atmosenv.2004.11.017, 2005.
- 520 Nelson, P. F., and Quigley, S. M.: The Hydrocarbon Composition Of Exhaust Emitted From Gasoline  
521 Fueled Vehicles, *Atmos. Environ.*, 18, 79-87, doi:10.1016/0004-6981(84)90230-0, 1984.
- 522 Ng, N. L., Herndon, S. C., Trimborn, A., Canagaratna, M. R., Croteau, P. L., Onasch, T. B., Sueper, D.,  
523 Worsnop, D. R., Zhang, Q., Sun, Y. L., and Jayne, J. T.: An Aerosol Chemical Speciation Monitor  
524 (ACSM) for Routine Monitoring of the Composition and Mass Concentrations of Ambient Aerosol,  
525 *Aerosol Sci. Tech.*, 45, 780-794, 2011.
- 526 Ogren, J. A., and Charlson, R. J.: Elemental Carbon in the Atmosphere-Cycle and Lifetime, *Tellus B.*,  
527 35, 241-254, 1983.
- 528 Parrish, D. D., and Zhu, T.: Clean Air for Megacities, *Science*, 326, 674-675,



- 529 doi:10.1126/science.1176064, 2009.
- 530 Qin, Y., Tonnesen, G. S., and Wang, Z.: Weekend/weekday differences of ozone, NO<sub>x</sub>, Co, VOCs,  
531 PM10 and the light scatter during ozone season in southern California, *Atmos. Environ.*, 38, 3069-  
532 3087, doi:10.1016/j.atmosenv.2004.01.035, 2004.
- 533 Schafer, H., Myronova, N., and Boden, R.: Microbial degradation of dimethylsulphide and related C-  
534 1-sulphur compounds: organisms and pathways controlling fluxes of sulphur in the biosphere, *J.*  
535 *Exp. Bot.*, 61, 315-334, doi:10.1093/jxb/erp355, 2010.
- 536 Schauer, J. J., Kleeman, M. J., Cass, G. R., and Simoneit, B. R. T.: Measurement of emissions from air  
537 pollution sources. 2. C-1 through C-30 organic compounds from medium duty diesel trucks, *Environ.*  
538 *Sci. Technol.*, 33, 1578-1587, doi:10.1021/Es980081n, 1999.
- 539 Schneider, J., Hock, N., Weimer, S., and Borrmann, S.: Nucleation particles in diesel exhaust:  
540 Composition inferred from in situ mass spectrometric analysis, *Environ. Sci. Technol.*, 39, 6153-  
541 6161, doi:10.1021/es049427m, 2005.
- 542 Shi, G. L., Liu, G. R., Tian, Y. Z., Zhou, X. Y., Peng, X., and Feng, Y. C.: Chemical characteristic and  
543 toxicity assessment of particle associated PAHs for the short-term anthropogenic activity event:  
544 During the Chinese New Year's Festival in 2013, *Sci. Total Environ.*, 482, 8-14,  
545 doi:10.1016/j.scitotenv.2014.02.107, 2014.
- 546 Singh, H., Chen, Y., Staudt, A., Jacob, D., Blake, D., Heikes, B., and Snow, J.: Evidence from the  
547 Pacific troposphere for large global sources of oxygenated organic compounds, *Nature*, 410, 1078-  
548 1081, doi:10.1038/35074067, 2001.
- 549 Stelson, A. W., and Seinfeld, J. H.: Relative-Humidity And Temperature-Dependence Of the  
550 Ammonium-Nitrate Dissociation-Constant, *Atmos. Environ.*, 16, 983-992, doi:10.1016/0004-  
551 6981(82)90184-6, 1982.
- 552 Subramanian, R., Kok, G. L., Baumgardner, D., Clarke, A., Shinozuka, Y., Campos, T. L., Heizer, C.  
553 G., Stephens, B. B., de Foy, B., Voss, P. B., and Zaveri, R. A.: Black carbon over Mexico: the effect  
554 of atmospheric transport on mixing state, mass absorption cross-section, and BC/CO ratios, *Atmos.*  
555 *Chem. Phys.*, 10, 219-237, doi:10.5194/acp-10-219-2010, 2010.
- 556 Sun, Y. L., Wang, Z. F., Fu, P. Q., Yang, T., Jiang, Q., Dong, H. B., Li, J., and Jia, J. J.: Aerosol  
557 composition, sources and processes during wintertime in Beijing, China, *Atmos. Chem. Phys.*, 13,  
558 4577-4592, doi:10.5194/acp-13-4577-2013, 2013.



- 559 Sun, Y. L., Wang, Z. F., Du, W., Zhang, Q., Wang, Q. Q., Fu, P. Q., Pan, X. L., Li, J., Jayne, J., and  
560 Worsnop, D. R.: Long-term real-time measurements of aerosol particle composition in Beijing,  
561 China: seasonal variations, meteorological effects, and source analysis, *Atmos. Chem. Phys.*, 15,  
562 10149-10165, doi:10.5194/acp-15-10149-2015, 2015.
- 563 Sun, Y. L., Wang, Z., Wild, O., Xu, W., Chen, C., Fu, P., Du, W., Zhou, L., Zhang, Q., Han, T., Wang,  
564 Q., Pan, X., Zheng, H., Li, J., Guo, X., Liu, J., and Worsnop, D. R.: "APEC Blue": Secondary  
565 Aerosol Reductions from Emission Controls in Beijing, *Sci. Rep.*, 6, 20668, doi:10.1038/srep20668,  
566 2016.
- 567 Tan, P. H., Chou, C., Liang, J. Y., Chou, C. C. K., and Shiu, C. J.: Air pollution "holiday effect" resulting  
568 from the Chinese New Year, *Atmos. Environ.*, 43, 2114-2124, doi:10.1016/j.atmosenv.2009.01.037,  
569 2009.
- 570 Wang, S.; Chai, F.; Xia, G.; Zhang, H.; Zhang, M.; Xue, Z.; Source Apportionment and Characteristics  
571 of SO<sub>2</sub> in Shenzhen City. *Res. Environ. Sci.*, 10 (22), 1128–1133, 2009 (in Chinese).
- 572 Wang, T., Nie, W., Gao, J., Xue, L. K., Gao, X. M., Wang, X. F., Qiu, J., Poon, C. N., Meinardi, S.,  
573 Blake, D., Wang, S. L., Ding, A. J., Chai, F. H., Zhang, Q. Z., and Wang, W. X.: Air quality during  
574 the 2008 Beijing Olympics: secondary pollutants and regional impact, *Atmos. Chem. Phys.*, 10,  
575 7603-7615, doi:10.5194/acp-10-7603-2010, 2010.
- 576 Wang, X. M., Sheng, G. Y., Fu, J. M., Chan, C. Y., Lee, S. G., Chan, L. Y., and Wang, Z. S.: Urban  
577 roadside aromatic hydrocarbons in three cities of the Pearl River Delta, People's Republic of China,  
578 *Atmos. Environ.*, 36, 5141-5148, doi:10.1016/S1352-2310(02)00640-4, 2002.
- 579 Xu, H. M., Tao, J., Ho, S. S. H., Ho, K. F., Cao, J. J., Li, N., Chow, J. C., Wang, G. H., Han, Y. M.,  
580 Zhang, R. J., Watson, J. G., and Zhang, J. Q.: Characteristics of fine particulate non-polar organic  
581 compounds in Guangzhou during the 16th Asian Games: Effectiveness of air pollution controls,  
582 *Atmos. Environ.*, 76, 94-101, doi:10.1016/j.atmosenv.2012.12.037, 2013.
- 583 Zhang, L., Shao, J. Y., Lu, X., Zhao, Y. H., Hu, Y. Y., Henze, D. K., Liao, H., Gong, S. L., and Zhang,  
584 Q.: Sources and Processes Affecting Fine Particulate Matter Pollution over North China: An Adjoint  
585 Analysis of the Beijing APEC Period, *Environ. Sci. Technol.*, 50, 8731-8740,  
586 doi:10.1021/acs.est.6b03010, 2016.
- 587 Zhang, Q., Worsnop, D. R., Canagaratna, M. R., and Jimenez, J. L.: Hydrocarbon-like and oxygenated  
588 organic aerosols in Pittsburgh: insights into sources and processes of organic aerosols, *Atmos. Chem.*



- 589 Phys., 5, 3289-3311, 2005.
- 590 Zhang, Q., Jimenez, J. L., Worsnop, D. R., and Canagaratna, M.: A case study of urban particle acidity  
591 and its influence on secondary organic aerosol, Environ. Sci. Technol., 41, 3213-3219,  
592 doi:10.1021/es061812j, 2007.
- 593 Zhang, Y. H., Hu, M., Zhong, L. J., Wiedensohler, A., Liu, S. C., Andreae, M. O., Wang, W., and Fan,  
594 S. J.: Regional Integrated Experiments on Air Quality over Pearl River Delta 2004 (PRIDE-  
595 PRD2004): Overview, Atmos. Environ., 42, 6157-6173, doi:10.1016/j.atmosenv.2008.03.025, 2008.
- 596 Zhao, J., Du, W. J., Zhang, Y. J., Wang, Q. Q., Chen, C., Xu, W. Q., Han, T. T., Wang, Y. Y., Fu, P. Q.,  
597 Wang, Z. F., Li, Z. S., and Sun, Y. L.: Insights into aerosol chemistry during the 2015 China victory  
598 day parade: results from simultaneous measurements at ground level and 260 m in Beijing, Atmos.  
599 Chem. Phys., 17, 1-29, doi:10.5194/acp-17-3215-2017, 2016.
- 600 Zheng, J. Y., Shao, M., Che, W. W., Zhang, L. J., Zhong, L. J., Zhang, Y. H., and Streets, D.: Speciated  
601 VOC Emission Inventory and Spatial Patterns of Ozone Formation Potential in the Pearl River Delta,  
602 China, Environ. Sci. Technol., 43, 8580-8586, doi:10.1021/es901688e, 2009.